

Two-Layer Shallow Water Equations with Momentum Conservative Scheme for Wave Propagation Simulation

Maria Artanta Ginting^{1*}, Dani Suandi², Yasi Dani³

¹⁻³Computer Science Department, School of Computer Science,
Bina Nusantara University,
Jakarta, Indonesia 11480
maria.ginting@binus.ac.id; dani.suandi@binus.edu;
yasi.dani@binus.ac.id

*Correspondence: maria.ginting@binus.ac.id

Abstract – In this paper, we discuss the implementation of momentum conservative scheme to shallow water equations (SWE). In shallow water model, the hydrodynamic pressure of the water is neglected. Here, the numerical calculation of mass and momentum conservation was applied on a staggered grid domain. The vertical interval was divided into two parts which made the computation quite efficient and accurate. Our focus is on the performance of the numerical scheme in simulating wave propagation and run-up phenomena, where the main challenge is to calculate the wave speed accurately and to count the non-linear term of the model. Here we also considered the wet and dry conditions of the topography. Three benchmark tests were picked out to validate the numerical scheme. A simulation of standing wave was carried out; the results were compared to the linear analytical solution and show a good fit. In addition, a simulation of harmonic wave propagation on a sloping beach was conducted, and the results closely align with the expected values from exact solution. Finally, we carried out a simulation of solitary wave with a sloping topography; and the results were compared to laboratory data. A good agreement was observed between the simulation results and experimental measurements.

Keywords: Shallow Water Equations; Momentum Conservative; Water Wave Simulation; Staggered Grid

I. INTRODUCTION

A more comprehensive knowledge of physical phenomena in shallow environments can be attained by studying the shallow water equations (SWE). Physical phenomena including standing waves (Anakhov, 2023; Ren et al., 2022), the generation of internal waves in straits (Cao et al., 2014; Kocaman et al., 2020; Qian et al., 2018), dam breaks (Cantero-Chinchilla et al., 2020; Chang et al., 2011), wave refraction (Hayatdavoodi & Ertekin, 2023), and tsunami propagation near the coast (Alfwzan et al., 2023; Tinh et al., 2021) have been extensively studied using SWE to understand their characteristics, behaviour, and impact. In the study of the shallow water model, the main assumption is that the horizontal length scale is much greater than the depth scale. This model is valid to simulate propagation of long wave, like tsunami. Furthermore, for problems with shorter wavelengths can be simulated using the Boussinesq approximation (Dai & Huang, 2021; Wang et al., 2023) and non-hydrostatic wave model (He et al., 2020; Ma et al., 2022).

In shallow water equations, the hydrodynamic pressure of the fluid is not taken into account. This condition results in faster numerical computation of this model. However, in numerical shallow water model, the challenge to be faced was in the discretization of the non-linear term, i.e. advection term in momentum equations. Here, we implemented the momentum conservative scheme to solve the shallow water equations numerically. A staggered grid domain was applied in this method (Stelling & Zijlema, 2003). The aim of this study is to validate the capability of numerical scheme in simulating various cases. Three test cases were conducted: standing wave phenomena,

harmonic and solitary wave run-up (Carrier & Greenspan, 1958; Synolakis, 1986). The standing wave simulation was carried out to validate the accuracy of the numerical scheme in calculating the wave velocity. Furthermore, the simulations of harmonic and solitary wave propagation on sloping topography were conducted to confirm the implementation of the wet-dry procedure.

Outline of this paper is described as follows. The explanation about mathematical model of the shallow water equations and the numerical methods are presented in Section 2. In Section 3, the results of numerical simulations are discussed. Finally, the conclusions are presented in Section 4.

II. METHODS

The shallow water equations are derived from Euler equations, which is a particular form of the Navier-Stokes equations for inviscid fluid with zero thermal conductivity. Consider a layer of fluid bounded above with a free surface $z=\eta(x,t)$ and below with a topography $z=-d(x)$. The two-dimensional Euler equations for homogeneous fluid are express as:

$$u_x + w_z = 0, \quad (1)$$

$$u_t + uu_x + ww_z = -g\eta_x - p_x, \quad (2)$$

$$w_t + uw_x + ww_z = -p_z, \quad (3)$$

where $u(x,z,t)$ and $w(x,z,t)$ respectively denotes the fluid particle velocity in horizontal and vertical direction, g the gravitational acceleration, and $p(x,z,t)$ the hydrodynamic pressure term. The total water thickness is denoted by $h(x,t)=\eta(x,t)+d(x)$.

In shallow water equations, the horizontal velocity $u(x,z,t)$ is calculated in terms of its depth averaged defined by:

$$\bar{u}(x,t) \equiv \frac{1}{h} \int_{-d}^{\eta} u(x,z,t) dz. \quad (4)$$

The horizontal domain is assumed to be much longer than the vertical domain, so the fluid vertical velocity can be ignored. The velocity at the surface is assumed to be equal to the velocity at the impermeable bottom, $u(x,z=\eta,t)=u(x,z=-d,t)=\bar{u}$. The integration of (1) over the fluid depth from $z=-d(x)$ to $z=\eta(x,t)$ leads to

$$h_t + (h\bar{u})_x = 0. \quad (5)$$

In shallow water assumption, the hydrodynamic pressure p is neglected. Thus, the governing equations for shallow water model are expressed as follows

$$h_t + (h\bar{u})_x = 0, \quad (6)$$

$$\bar{u}_t + \bar{u}\bar{u}_x + g\eta_x = 0. \quad (7)$$

Now consider the equations (1-3), where the total fluid depth is divided into two-layer, $h_1(x,t)$ and $h_2(x,t)$ with $h(x,t)=h_1(x,t)+h_2(x,t)$. The water thickness at upper layer is denoted by $h_1(x,t)$ and at lower layer is denoted by $h_2(x,t)$. Here h_1 and h_2 are not necessarily equal. The governing

equations for two-layer shallow water model are:

$$h_t + \partial_x (h_1 \bar{u}_1) + \partial_x (h_2 \bar{u}_2) = 0, \quad (8)$$

$$\partial_t (\bar{u}_1) + \bar{u}_1 \partial_x (\bar{u}_1) + g \partial_x \eta = 0, \quad (9)$$

$$\partial_t (\bar{u}_2) + \bar{u}_2 \partial_x (\bar{u}_2) + g \partial_x \eta = 0. \quad (10)$$

These equations will be solved numerically using momentum conservative scheme in staggered grid, which is adopted from Stelling and Zijlema (2003).

In this method the horizontal grid is defined by:

$$\{0=x_{(1/2)}, x_1, x_{(3/2)}, x_2, \dots, x_N, x_{(N+1/2)} = L\}. \quad (11)$$

In this domain, the unknowns are arranged as in Figure 1. The horizontal velocity is located at the center of the cell, and the water height is located at the edge of the cell.

Since the water height is computed at the edge of the cell, the value of h at the centre of the cell is calculated using upwind approximation, which is denoted with, *h and defined by:

$${}^*h_{i+\frac{1}{2}}^n = \begin{cases} h_i^n & \text{if } (\bar{u}_{1,i+\frac{1}{2}}^n + \bar{u}_{2,i+\frac{1}{2}}^n) > 0 \\ h_{(i+1)}^n & \text{if } (\bar{u}_{1,i+\frac{1}{2}}^n + \bar{u}_{2,i+\frac{1}{2}}^n) < 0 \\ \max(\eta_i^n, \eta_{i+1}^n) + \min(d_i, d_{i+1}) & \text{if } (\bar{u}_{1,i+\frac{1}{2}}^n + \bar{u}_{2,i+\frac{1}{2}}^n) = 0. \end{cases} \quad (12)$$

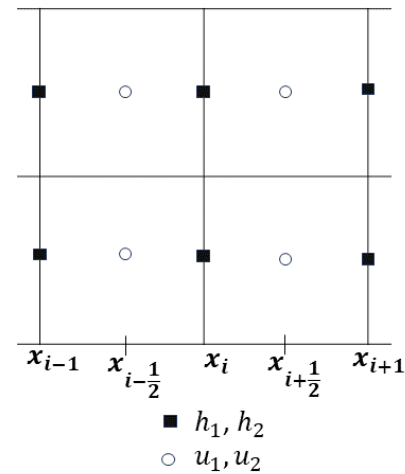


Figure 1 The Unknowns Position in Staggered Grid Domain

This approximation follows the water flow direction. Thus, the discrete equations from (8-10) can be written as follows.

$$\frac{h_i^{n+1} - h_i^n}{\Delta t} + \frac{{}^*h_{i+\frac{1}{2}}^n \bar{u}_{1,i+\frac{1}{2}}^n - {}^*h_{i-\frac{1}{2}}^n \bar{u}_{1,i-\frac{1}{2}}^n}{2\Delta x} + \frac{{}^*h_{i+\frac{1}{2}}^n \bar{u}_{2,i+\frac{1}{2}}^n - {}^*h_{i-\frac{1}{2}}^n \bar{u}_{2,i-\frac{1}{2}}^n}{2\Delta x} = 0, \quad (13)$$

$$\frac{\bar{u}_{m,i+\frac{1}{2}}^{n+1} - \bar{u}_{m,i+\frac{1}{2}}^n}{\Delta t} + \bar{u}_m \partial_x \bar{u}_m |_{i+\frac{1}{2}}^n + g \left(\frac{\eta_{i+1}^n - \eta_i^n}{\Delta x} \right) = 0, \quad (14)$$

for $m = 1, 2$. The momentum equations above are calculated when the cell $[x_{(i-1)}, x_i]$ is wet, that is when $h_{i-1} > 0$ and $h_i > 0$ are satisfied. Here, the advection terms $\bar{u} \partial_x \bar{u}$ are approximated using momentum conservative scheme which is derived in Stelling and Busnelli (2001), as follows

$$\begin{aligned} & (\bar{u} \partial_x \bar{u})_{m,i-1/2} \\ &= \frac{1}{\bar{h}_{m,i-1/2}} \left(\frac{\bar{q}_{m,i} u_{m,i}^* - \bar{q}_{m,i} u_{m,i-1}^*}{\Delta x} \right. \\ & \quad \left. - \bar{u}_{m,i-1/2} \frac{\bar{q}_{m,i} - \bar{q}_{m,i-1}}{\Delta x} \right) \end{aligned} \quad (15)$$

where:

$$\bar{h}_{m,i-1/2} = \frac{1}{2} (h_{m,i-1} + h_{m,i}), \quad (16)$$

$$\bar{q}_{m,i} = \frac{1}{2} \left(q_{m,i+1/2} - q_{m,i-1/2} \right), \quad (17)$$

$$q_{m,i-1/2} = h_{m,i-1/2} \bar{u}_{m,i-1/2}, \quad (18)$$

$$u_{m,i}^* = \begin{cases} \bar{u}_{m,i-1/2} & \text{if } \bar{q}_{m,i} \geq 0 \\ \bar{u}_{m,i+1/2} & \text{if } \bar{q}_{m,i} < 0. \end{cases} \quad (19)$$

III. RESULTS AND DISCUSSION

This section describes three test problems to validate the numerical scheme. The first test case is a standing wave simulation on flat bottom. In this case, the wave propagation that is produced by the numerical simulation is compared to the exact solution. Other cases are conducted to test the wet-dry procedure, i.e. harmonic and solitary wave run-up on sloping beach.

3.1 Simulation of Standing Wave

The first test case is standing wave simulation in a closed basin. In this simulation, we chose the length 100 m and depth 5 m. The initial wave height was taken as:

$$\eta(x,0) = A \cos(kx), \quad (20)$$

where the amplitude $A = 0.1$, the wave number $k = \pi/100$, and $0 \leq x \leq 100$. In numerical computation, the horizontal domain was divided into 1000 grid cells of each 0.1 m, and the computation time step was 0.01 s.

Here we compare the numerical result to the exact solution. Figure 2 presents the comparison of time series of two-layer SWE and exact surface elevation at $x=75$ m. The simulation (blue solid line) and exact solution (red dotted line) show a very good agreement. The waves from our computed simulation are able to propagate at almost the same speed as the exact solution. The exact solution is obtained from linear wave theory:

$$\begin{aligned} \eta(x,t) = & 0.05 \left(\cos \left(\frac{\pi}{100} (x - 2.21t) \right) \right. \\ & \left. + \cos \left(\frac{\pi}{100} (x + 2.21t) \right) \right) \end{aligned} \quad (21)$$

And the wave propagation speed, $c=2.21$, is calculated based exact linear dispersion relation:

$$c = \frac{\omega}{k} = \sqrt{\frac{g}{k} \tanh(kd)}. \quad (22)$$

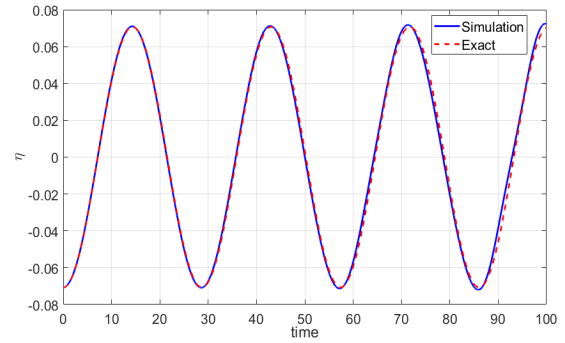


Figure 2. Comparison of Wave Surface at $x = 75$ Between Numerical Simulation and Exact Solution

3.2 Harmonic Wave Run-up

In this case, we simulate propagation of harmonic wave on a sloping beach. This case is also known as Carrier-Greenspan (1958) problem. The computation is carried out at domain $-12.5 \leq x \leq 5$, where the bottom topography is a beach with slope 1:25 and the maximum depth is 0.5 m. Spatial discretization $\Delta x = 0.02$ m and time step $\Delta t = 0.006$ s are used in the numerical computation.

The simulation result is presented in Figure 3 below. Here we compare the shoreline motion simulated using two-layer SWE (blue line) and the analytical solution from Carrier and Greenspan (red dotted line). However, the analytical solution is derived using SWE model. This result show that our numerical scheme is able to predict the wave run-up and to count the wet-dry condition in this case well.

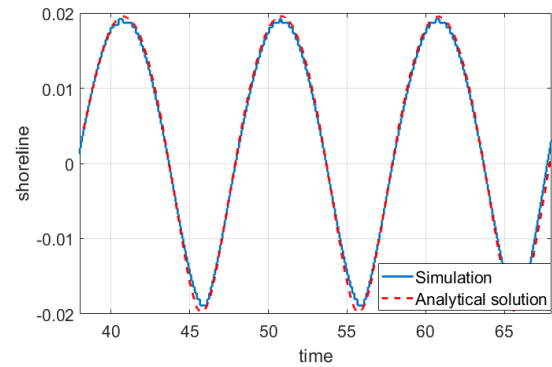


Figure 3. Shoreline Motion of Carrier and Greenspan Problem

3.3 Solitary Wave on Sloping Beach

The last test case is a simulation of solitary wave on sloping beach. This simulation is conducted based on an experiment by Synolakis (1987) in W. M. Keck Laboratory, California Institute of Technology. The experiment was carried out as a validation of linear wave theory, derived by Synolakis, to predict the maximum run-up of solitary wave on sloping beach. In the laboratory, a wave tank with length 37.73 m, width 0.61 m, and height 0.39 m was used, with a sloping beach (with slope 1:19.85) at the right side of the tank.

The initial wave is a solitary wave with peak at $x = X_1$ as follow:

$$\eta(x,0) = A/d \operatorname{sech}^2 \gamma (x - X_1), \quad (23)$$

where $\gamma = (3A/4d)^{1/2}$ and A/d is normalized amplitude of solitary wave. In this case, we use $A/d = 0.0185$, with computational discretization $\Delta x = 0.2$ and $\Delta t = 0.01$. The computational domain is $x \in [-300, 10]$. The results are shown in Figure 4. We present the wave profile at four different dimensionless time, they are at $t = 40$, $t = 50$, $t = 60$ and $t = 70$. These numerical results (blue solid line) are compared to the laboratory results (red dotted line). In general, the comparison shows a good agreement, especially during the wave run-up.

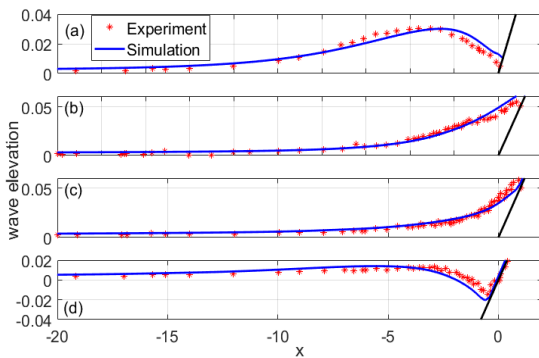


Figure 4. Wave Profile at (a) $t = 40$, (b) $t = 50$, (c) $t = 60$, (d) $t = 70$

IV. CONCLUSION

In this present study, the numerical scheme of momentum conservative on staggered grid has been successfully implemented on shallow water equations. In this model, the non-hydrostatic pressure term is ignored. The two-layer numerical model produced good results in simulating standing wave phenomena and harmonic and solitary wave propagation over a sloping beach, including predicting wave run-up height. The results of simulations are compared to exact theory or laboratory data. In our numerical scheme, we also implemented the wet-dry procedure for the wave run-up cases. Validation and verification of this numerical scheme with more various cases invites further exploration.

REFERENCES

- Alfwzan, W., Yao, S. W., Allehiyany, F. M., Ahmad, S., Saifulah, S., & Inc, M. (2023). Analysis of fractional non-linear tsunami shallow-water mathematical model with singular and non singular kernels. *Results in Physics*, 52. <https://doi.org/10.1016/j.rinp.2023.106707>
- Anakhov, P. (2023). Excitation of an extreme wave by standing current. *Oceanologia*, 65(4). <https://doi.org/10.1016/j.oceano.2023.06.005>
- Cantero-Chinchilla, F. N., Bergillos, R. J., Gamero, P., Castro-Orgaz, O., Cea, L., & Hager, W. H. (2020). Vertically averaged and moment equations for dam-break wave modeling: Shallow water hypotheses. *Water (Switzerland)*, 12(11). <https://doi.org/10.3390/w12113232>
- Cao, Z., Huang, W., Pender, G., & Liu, X. (2014). Even more destructive: Cascade dam break floods. *Journal of Flood Risk Management*, 7(4). <https://doi.org/10.1111/jfr3.12051>
- Chang, T. J., Kao, H. M., Chang, K. H., & Hsu, M. H. (2011). Numerical simulation of shallow-water dam break flows in open channels using smoothed particle hydrodynamics. *Journal of Hydrology*, 408(1–2). <https://doi.org/10.1016/j.jhydrol.2011.07.023>
- Dai, A., & Huang, Y. L. (2021). Boussinesq and non-Boussinesq gravity currents propagating on unbounded uniform slopes in the deceleration phase. *Journal of Fluid Mechanics*, 917. <https://doi.org/10.1017/jfm.2021.300>
- Hayatdavoodi, M., & Ertekin, R. C. (2023). Diffraction and Refraction of Nonlinear Waves by the Green-Naghdi Equations. *Journal of Offshore Mechanics and Arctic Engineering*, 145(2). <https://doi.org/10.1115/1.4055484>
- He, D., Ma, Y., Dong, G., & Perlin, M. (2020). Predicting deep water wave breaking with a non-hydrostatic shock-capturing model. *Ocean Engineering*, 216. <https://doi.org/10.1016/j.oceaneng.2020.108041>
- Kocaman, S., Güzel, H., Evangelista, S., Ozmen-Cagatay, H., & Viccione, G. (2020). Experimental and numerical analysis of a dam-break flow through different contraction geometries of the channel. *Water (Switzerland)*, 12(4). <https://doi.org/10.3390/W12041124>
- Ma, Y. X., Ai, C. F., & Dong, G. H. (2022). A REVIEW ON NON-HYDROSTATIC WATER WAVE MODELS. In *Oceanologia et Limnologia Sinica* (Vol. 53, Issue 4). <https://doi.org/10.11693/hyh20220200041>
- Qian, H., Cao, Z., Liu, H., & Pender, G. (2018). New experimental dataset for partial dam-break floods over mobile beds. In *Journal of Hydraulic Research* (Vol. 56, Issue 1). <https://doi.org/10.1080/00221686.2017.1289264>
- Ren, Z., Liu, H., Jimenez, C., & Wang, Y. (2022). Tsunami resonance and standing waves in the South China Sea. *Ocean Engineering*, 262. <https://doi.org/10.1016/j.oceaneng.2022.112323>
- Stelling, G., & Zijlema, M. (2003). An accurate and efficient finite-difference algorithm for non-hydrostatic free-surface flow with application to wave propagation. *International Journal for Numerical Methods in Fluids*, 43(1). <https://doi.org/10.1002/fld.595>
- Tinh, N. X., Tanaka, H., Yu, X., & Liu, G. (2021). Numerical implementation of wave friction factor into

the 1D tsunami shallow water equation model. *Coastal Engineering Journal*, 63(2). <https://doi.org/10.1080/21664250.2021.1919391>

Wang, Z. A., Yang, A., & Zhao, K. (2023). Wave propagation and stabilization in the Boussinesq–Burgers system. *Physica D: Nonlinear Phenomena*, 447. <https://doi.org/10.1016/j.physd.2023.133687>